Recent Advances in MEMS-VCSELs for High Performance Structural and Functional SS-OCT Imaging

V. Jayaraman[a], D.D. John[a], C. Burgner[a], M.E. Robertson[a], B. Potsaid[b], J.Y. Jiang[b], T.H. Tsai[c], W. Choi[c], C.D. Lu[c], P.J.S. Heim[b], J.G. Fujimoto[c], and A.E. Cable[b].
a. Praevium Research, Inc. 5385 Hollister Avenue #211 Building 8, Office 16, Santa Barbara, CA 93111, USA. b. Thorlabs, Inc., 56 Sparta Avenue Newton, NJ 07860, USA. c. Department of Electrical and Computer Engineering, Massachusetts Institute of Technology, 77 Massachusetts Avenue, Cambridge, MA 02139, USA.

ABSTRACT

Since the first demonstration of swept source optical coherence tomography (SS-OCT) imaging using widely tunable micro-electromechanical systems vertical cavity surface-emitting lasers (MEMS-VCSELs) in 2011, VCSEL-based SS-OCT has advanced in both device and system performance. These advances include extension of MEMS-VCSEL center wavelength to both 1060nm and 1300nm, improved tuning range and tuning speed, new SS-OCT imaging modes, and demonstration of the first electrically pumped devices. Optically pumped devices have demonstrated continuous single-mode tuning range of 150nm at 1300nm and 122nm at 1060nm, representing a fractional tuning range of 11.5%, which is nearly a factor of 3 greater than the best reported MEMS-VCSEL tuning ranges prior to 2011. These tuning ranges have also been achieved with wavelength modulation rates of >500kHz, enabling >1 MHz axial scan rates. In addition, recent electrically pumped devices have exhibited 48.5nm continuous tuning range around 1060nm with 890kHz axial scan rate, representing a factor of two increase in tuning over previously reported electrically pumped MEMS-VCSELs in this wavelength range. New imaging modes enabled by optically pumped devices at 1060nm and 1300nm include full eye length imaging, pulsatile Doppler blood flow imaging, high-speed endoscopic imaging, and hand-held wide-field retinal imaging.

Keywords: Optical coherence tomography, MEMS-VCSELs, Tunable lasers, Biomedical Imaging

I. INTRODUCTION

Rapidly swept, widely tunable lasers have long been recognized as a critical enabling technology in swept source optical coherence tomography (SS-OCT)[1, 2]. A comprehensive review of swept source options is found in Table I of a recent publication on ophthalmic imaging[3]. Since 2011, amplified micro-electromechanical systems tunable vertical–cavity surface-emitting lasers (MEMS-VCSELs) have emerged as a high performance swept source for SS-OCT, providing a unique combination of wide tuning range, high and variable sweep speed, long dynamic coherence length, high output power, and wavelength flexibility[4, 5]. The high sweep rate of these devices has enabled real-time acquisition of large volumetric data sets, reduced sensitivity to patient motion, and imaging of dynamically varying physiological processes. High power levels have enabled excellent imaging in both endoscopic and ophthalmic applications. The variable sweep rate has enabled both long range lower-speed imaging and short range higher-speed imaging with a single MEMS-VCSEL device, demonstrated for example in ophthalmic applications[3], but likely of utility in many other imaging scenarios.

Although MEMS-VCSELs were first conceived in the mid 1990's[6, 7], development efforts in the field until 2009 were driven primarily by telecommunications and narrow-tuning spectroscopic applications[8-10]. In 2009, Praevium Research, Advanced Optical Microsystems, commercial partner Thorlabs, and academic partner Massachusetts Institute of Technology (MIT) began developing a swept source based on amplified MEMS-VCSELs, targeting SS-OCT as a primary application. This work was motivated by several factors. First, the large free-spectral range (FSR) of a VCSEL cavity promised continuous single-mode tuning, in contrast to other swept sources that tuned a cluster of modes[11] or tuned by mode-hopping[12, 13]. This suggested that the VCSEL would have superior dynamic coherence length. Additionally, the very short VCSEL cavity also suggested very fast laser dynamics and the possibility of unprecedented sweep speeds.

Optical Coherence Tomography and Coherence Domain Optical Methods in Biomedicine XVIII, edited by Joseph A. Izatt, James G. Fujimoto, Valery V. Tuchin, Proc. of SPIE Vol. 8934, 893402 · © 2014 SPIE · CCC code: 1605-7422/14/$18 · doi: 10.1117/12.2041718

In 2011, we reported the first widely tunable optically pumped 1300nm MEMS-VCSELs, exhibiting 110nm tuning range, and demonstrated SS-OCT imaging with these devices up to an axial scan rate of 760kHz[14]. Since that time, optically pumped 1060nm devices have also been developed[15], the tuning range at both 1060 and 1300nm[16] has increased, and a large number of imaging results have been demonstrated at both wavelengths. In recent months, we have also demonstrated the widest tuning range to date in electrically pumped 1060nm MEMS-VCSELs. The sections below review these most recent results in greater detail.

2. OPTICALLY PUMPED 1300NM AND 1060NM VCSEL DEVICE PERFORMANCE

Figure 1 below illustrates the basic components of an SS-OCT swept source based on optically pumped MEMS-VCSELs, including the MEMS-VCSEL itself, pump laser and isolator, semiconductor optical amplifier, and the tuning signal generator which drives the MEMS actuator. The wavelength division multiplexer (WDM) separates incoming pump light from outgoing tuned MEMS-VCSEL emission. The 1060nm MEMS-VCSEL employs an 850nm optical pump, while the 1300nm MEMS-VCSEL employs a 980nm optical pump. Typical post-amplified powers are 15-25 mW at 1060nm and 30-60mW at 1300nm. Figure 2 illustrates the VCSEL device structure used at both 1060nm and 1300nm, while figures 3 and 4 summarize the best device results obtained at these two wavelengths.

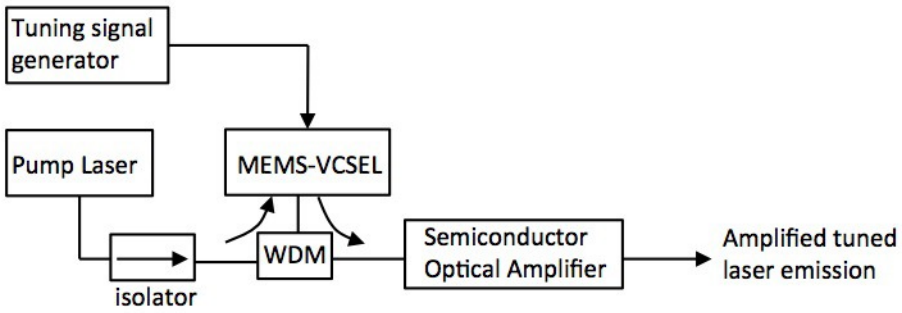

Figure 1: Basic components of optically pumped MEMS-VCSEL for Swept-Source OCT (SS-OCT) imaging. A pump laser provides energy to optically pump the MEMS-VCSEL gain region, through a WDM coupler, which separates incoming pump light from outgoing MEMS-VCSEL tuned light. The MEMS-VCSEL output is amplified through a semiconductor optical amplifier, generating amplified tuned laser emission of 15-25mW at 1060nm and 25-60mW at 1300nm. A tuning signal generator provides an arbitrary voltage waveform to drive the MEMS actuator.

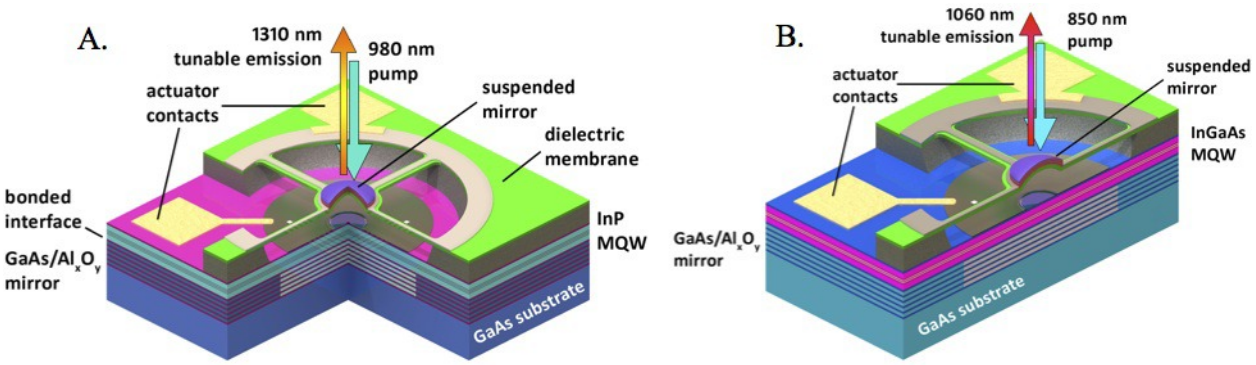

Figure 2: MEMS-VCSEL device structures at 1300nm (A)[16] and 1060nm (B)[15]. Both devices employ a fully oxidized GaAs/AlxOy bottom mirror, multi-quantum well gain region and suspended top mirror. The 1300nm device employs wafer bonding to combine the InP-based multi-quantum well with the GaAs-based mirror region. The 1060 device integrates gain region and mirror in one epitaxial growth step. Application of a voltage across the actuator contacts in both devices contracts the air-gap and tunes the laser emission to shorter wavelengths.

As shown in Fig. 2, the 1060nm device structure employs an InGaAs multi-quantum well (MQW) gain medium combined in one epitaxial growth step with a fully oxidized GaAs/AlxOy[17] mirror structure. The 1300nm structure

requires GaAs to InP wafer bonding[18-20] to combine the InP-based multi-quantum well active region with the GaAs-based broadband fully oxidized mirror.

Both devices employ a top suspended dielectric mirror separated from the underlying gain region and bottom mirror by a ~1-2μm air-gap. Application of a voltage between the suspended membrane and fixed underlying structure contracts the air-gap through electrostatic force and tunes the laser to shorter wavelengths. Contracting the air-gap half a wavelength sweeps the laser wavelength through one full free spectral range (FSR) which is typically >100nm at both 1060nm and 1300nm. In addition, through proper design of layer thicknesses, layer stresses, and actuator shape, it is possible to repeatably achieve MEMS resonances of several hundred kHz, and therefore wavelength sweep rates in this range or greater.

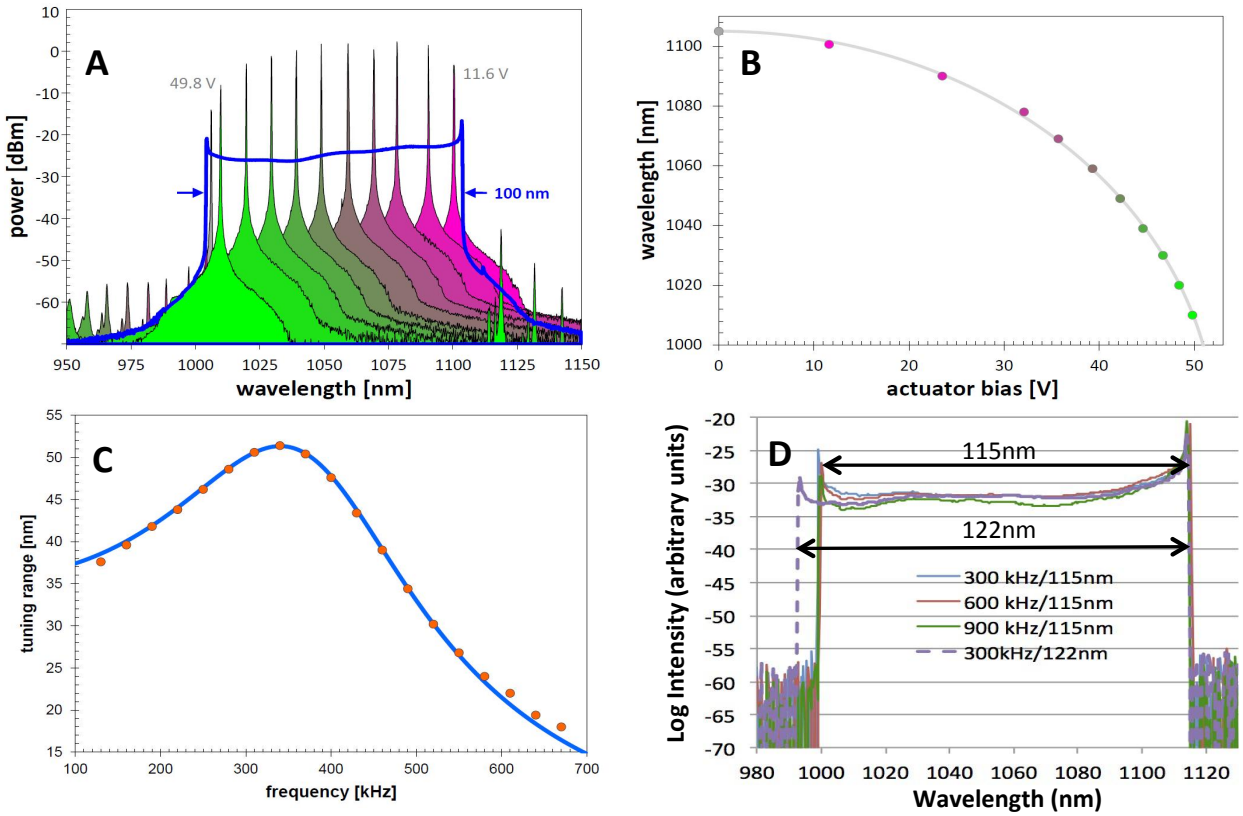

Figure 3: Summary of most relevant 1060nm MEMS-VCSEL results. Results shown in A-C represent a device generation from late 2012[15], while tuning results in Fig. 3D represent most recent results expanding the tuning range by 22%. A. Demonstration of both 90nm static and 100nm dynamic tuning range near 1060nm. The dynamic tuning range was obtained under 400kHz sinusoidal drive, and is the more relevant tuning range for SS-OCT. B. Wavelength vs. voltage applied to MEMS actuator. The dots represent measured data, and the solid line represents theory. C. Typical MEMS frequency response for 1060nm MEMs devices, exhibiting 350 kHz resonance and slightly under-damped response. D. Four time-averaged spectra under sinusoidal drive, taken with a single device from a recent generation designed for wider tuning range in late 2013. As shown, this device exhibited a maximum tuning range of 122nm (dashed spectrum), representing a fractional tuning range 122/1060nm of 11.5%. The same device also demonstrated no significant change when held at 115nm tuning range and driven with higher voltages at 600 and 900kHz to maintain the 115nm bandwidth (solid spectra).

Figure 3 summarizes the best 1060nm device results obtained using the structure of Figure 2B. Figures 3A-C demonstrate results obtained in 2nd generation devices reported in late 2012[15], demonstrating 100nm dynamic tuning range, 90nm static tuning range, and operating voltage on the order of 50-60 Volts at full tuning. These devices also demonstrated MEMS resonance frequencies around 350 kHz (3C). Figure 3D shows the most recent results obtained in late 2013, in which tuning range has been expanded to a maximum of 122nm around 1060nm. Another notable feature of the device in Figure 3D is the demonstrated ability of the device to operate up to 900kHz with no discernible laser degradation, demonstrating the fast dynamics of the laser cavity. As shown, time-averaged spectra obtained with

sinusoidal drive at 300,600, and 900 kHz, while tuning over 115nm bandwidth, show nearly identical characteristics, although drive voltages must be significantly increased at the higher frequencies to maintain optical bandwidth well beyond the ~350kHz mechanical resonance. Operation at even higher rates is possible, but requires peak voltages exceeding the capability of the voltage source employed. The ability of the VCSEL to operate at ~MHZ repetition rates (900kHz corresponding to 1.8MHz axial scan rate with bi-directional scanning), is in contrast to other swept sources using longer external cavity designs[2].

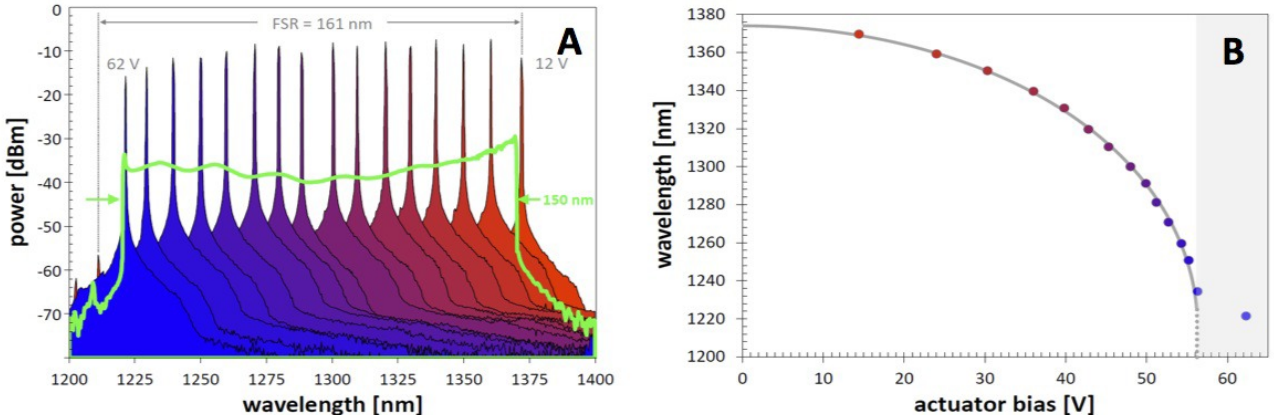

Figure 4: Summary of most relevant 1300nm MEMS-VCSEL device results[16]. A. 150nm dynamic tuning achieved at a center wavelength of 1300nm and 500kHz sinusoidal drive, representing a fractional tuning range of 150/1300=11.5%. B. Applied voltages on the order of 60V for full tuning. The best device results of Figs. 4A-B have not yet reached commercialization.

Figure 4 illustrates the best 1300nm device results achieved. The 150nm tuning range was first reported in 2012[16], with voltages on the order of 60V for full tuning. Since that time, emphasis on these devices has been on demonstrating reliability and manufacturability, leading to the commercialization of 1310nm devices in 2013. Commercial devices exhibit >100nm tuning range, with the best research results to date exhibiting 150nm of tuning. We note that the fractional tuning range obtained with best research results (150nm/1300nm=11.5%, similar to 122nm/1060nm=11.5%) represents nearly a factor of 3 increase over the best MEMS-VCSELs reported prior to 2011 (65nm/1550nm=4.2%)[8]. In addition to our results, another group in 2011 also reported 102nm tuning range in a 1550nm VCSEL using slower electro-thermal tuning at ~hundreds of Hz[21], and 74nm at 1550nm using faster electrostatic MEMS tuning up to 215 kHz[22].

3. IMAGING WITH OPTICALLY PUMPED MEMS-VCSELs

Over the last two years, optically pumped MEMS-VCSELs have enabled improved SS-OCT imaging performance and demonstration of new imaging modes difficult to achieve with other swept sources. Figures 5-9 summarize some key results of the last two years, all of which were obtained by our collaborators in the OCT imaging group at the Massachusetts Institute of Technology. These results rely on various features of the MEMS-VCSEL, most importantly on long coherence length, fast imaging speed, and phase stability. The details of imaging are presented in other publications; the purpose of this section is to overview the breadth of SS-OCT results enabled by MEMS-VCSEL technology.

Figure 5 illustrates whole eye imaging obtained with the 1060nm MEMS-VCSEL in late 2012[3], demonstrating imaging from the anterior eye through the retina with one MEMS-VCSEL-based swept source, enabled by the long VCSEL coherence length. This coherence length has been exploited to make axial eye length measurements, which have compared well with clinically established optical and ultra-sound bio-meters[23].

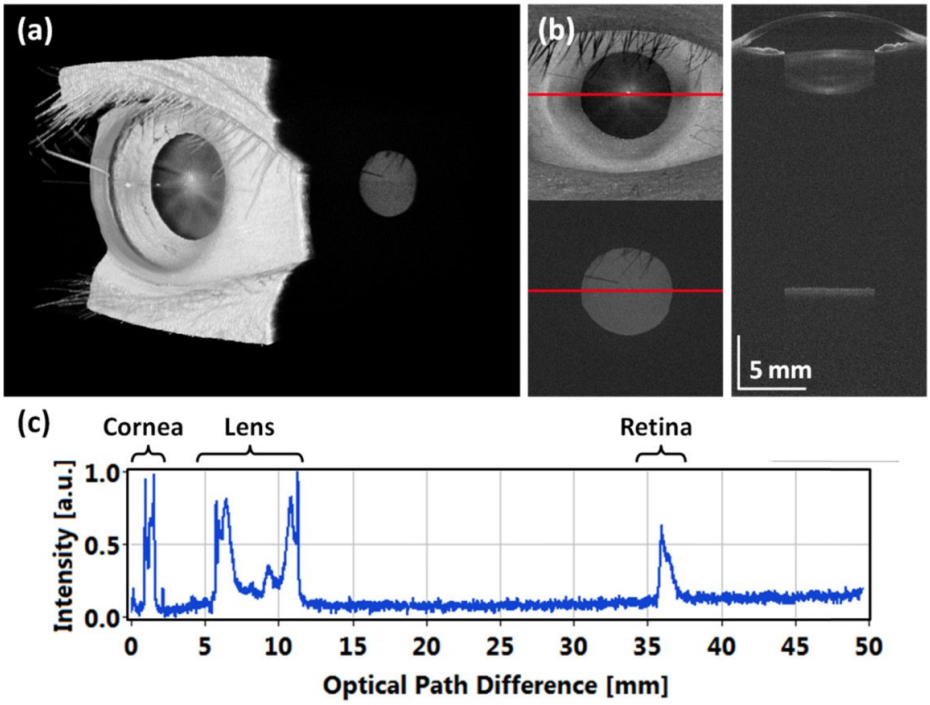

Figure 5: Whole eye image obtained with 1060nm MEMS-VCSEL, illustrating imaging of the anterior eye and retina in a single acquisition (~40mm imaging range), enabled by the long coherence length of the VCSEL[3]. Axial eye length measurements using this long-range OCT have compared favorably with clinical optical and ultrasound biometers.

Figure 6 illustrates pulsatile Doppler blood flow imaging of a retinal arterial network using the 1060nm MEMS-VCSEL, demonstrating measurement of axial blood velocity at different times within a cardiac cycle, enabled by the 400kHz axial scan rate and phase stability of the MEMS-VCSEL[24]. Figures 6C-F illustrate blood velocity contrast at different times within one cardiac cycle, represented by the 4 arrows in Figure 6A.

Figure 7 below shows a hand-held SS-OCT system used for portable wide-field retinal imaging[25]. The 1060nm MEMS-VCSEL employed in this system operates at 350kHz axial scan rate, which, together with a motion correction imaging algorithm, enables excellent imaging in the hand-held configuration. Figures 7A-D illustrate the structure of two hand-held designs. Figure 7E illustrates an en-face retinal image, while Figs. 7F-I illustrate cross-sections through the various dashed lines. Figure 7H and 7I illustrate a cross-section along the dashed yellow line with and without motion correction, respectively, illustrating the elimination of motion artifacts via the motion correction algorithm.

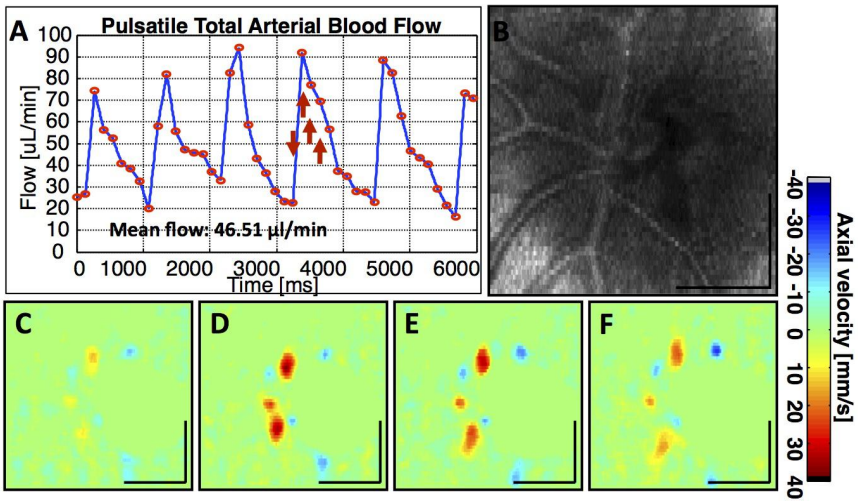

Figure 6: Doppler blood flow imaging at 400 kHz axial scan rate[24]. Scale bars represent 500µm. A. Pulsatile total arterial blood flow, illustrating flow variation within cardiac cycle. B. En face OCT projection image of retinal arterial network. C-F. En face Doppler images taken at different times represented by the 4 arrows in 6A, illustrating the ability of Doppler OCT with 1060nm MEMS-VCSEL to resolve axial blood velocity at different times within a cardiac cycle.

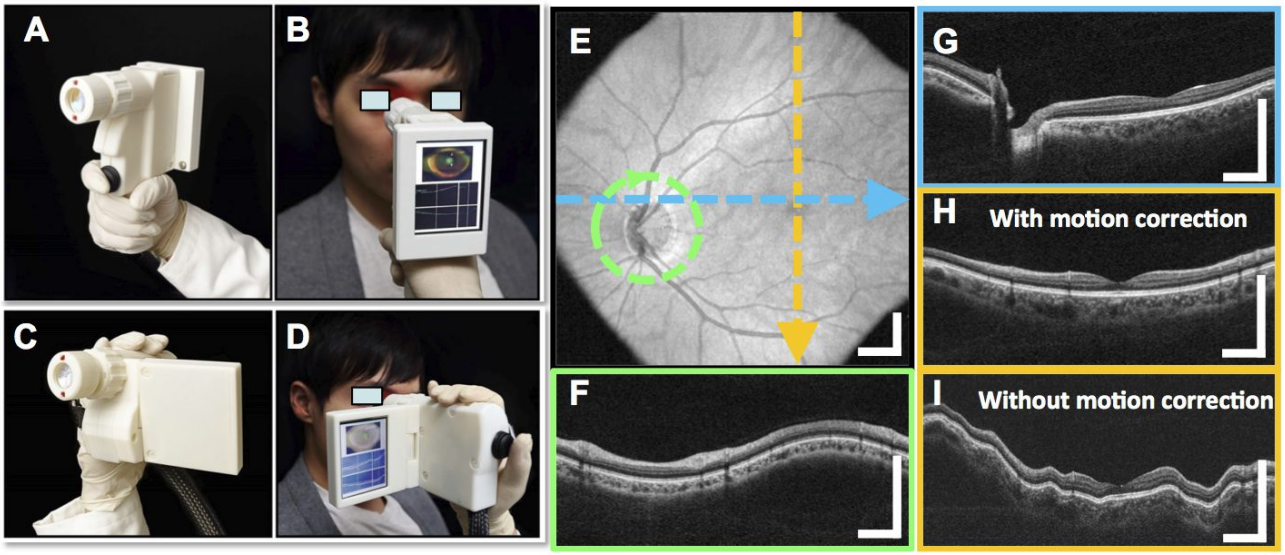

Figure 7: Hand-held wide-field retinal imaging and associated imaging results[25]. Figs. A-D illustrate two hand-held designs. E. En face retinal image. F. Circular cross-section along green dashed line. G. Cross-section along dashed blue line. H. Cross-section along dashed yellow line with motion correction. I. Cross-section along dashed yellow line without motion correction, illustrating motion artifacts.

Figure 8 below illustrates ex-vivo endoscopic volumetric imaging of the human colon.[26] The images shown were acquired using a 1300nm MEMS-VCSEL operating at 1 MHz axial scan over a 107nm wavelength sweep range. Tuned emission from the VCSEL entered the colon through a micro-motor based imaging catheter, shown in Figure 9, which employed 24,000 RPM and 1mm/sec pullback rate to acquire images at 400 frames per second, 2.5µm separation per frame, and 8µm axial and transverse resolution in tissue.

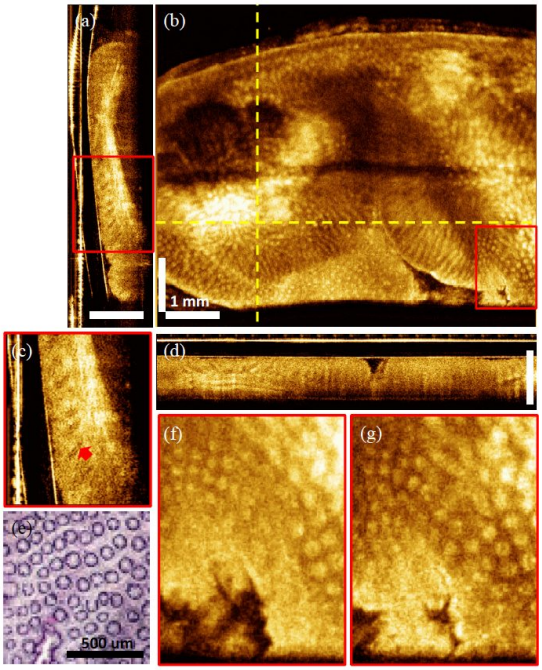

Figure 8: Ex-vivo endoscopic imaging of the human colon[26]. A. Cross-sectional image along rotary direction. B. En face image at 350μm imaging depth. C. Enlarged view of the red box in (A). D. Cross-sectional view along pullback direction. E. Representative en face histology with hematoxylin and eosin stain. F. Enlarged image at same area as red box in (B), at 250μm imaging depth. G. Enlarged image of same area as in red box in (B), at 350μm imaging depth.

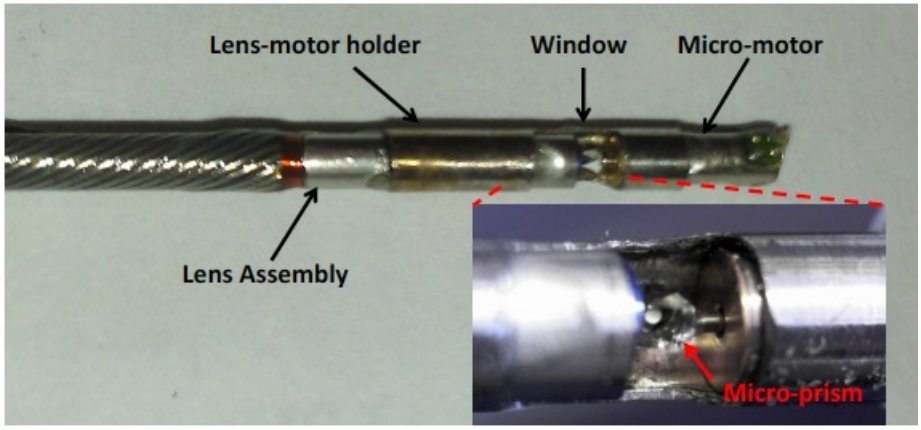

Figure 9: Micro-motor based imaging catheter developed for high-speed endoscopic imaging shown in Fig. 8[26]. The rotating microprism reflects the OCT beam and focuses it outside the catheter sheath to image the colon.

The images shown in Figs. 5-8 represent a sampling of the results obtained with MEMS-VCSEL based SS-OCT, illustrating an expanding breadth of applications impacted by this technology. One area of emerging interest not represented in Figs. 5-8 is OCT angiography using high-speed VCSELs, which has recently enabled in-vivo wide-field imaging of fine choroidal and choriocapillaris microvascular structure with no exogenous contrast agent[27]. OCT angiography using VCSELs uses speckle de-correlation between multiple B-scans at a fixed location to visualize erythrocyte motion. This visualization has the potential to aid the diagnosis of retinal diseases such as age-related macular degeneration and diabetic retinopathy.

Another area of SS-OCT imaging with MEMS-VCSELs not represented in Figs. 5-8 is extremely long range imaging. Although ophthalmic whole-eye imaging demonstrates the >35mm imaging range of the MEMS-VCSEL, the actual imaging range and VCSEL coherence length is much larger. This has been demonstrated by the MIT group in imaging multi-centimeter solid objects and by using the swept MEMS-VCSEL to measure fiber lengths exceeding one meter[28]. The ultra-long dynamic coherence length remains to be fully quantified, since measuring coherence length under swept operation requires prohibitively fast detection electronics to resolve the rapidly varying fringes. By restricting tuning range to ~1nm and using slow scan rates, however, it is possible to measure coherence lengths exceeding ten meters. This is consistent with an intrinsic laser linewidth of a few MHz. This exceptional coherence length will be the subject of a future publication and is likely to enable as-yet unexplored imaging and sensor applications.

4. ELECTRICALLY PUMPED 1060NM MEMS-VCSELS

The demonstration of optically pumped wide tuning range MEMS-VCSELs at both 1060nm and 1300nm, along with demonstrations of high-quality SS-OCT imaging and new imaging modes, has validated the MEMS-VCSEL as a powerful swept-source technology in SS-OCT imaging systems. VCSEL technology also has the potential to drive down the cost of SS-OCT systems, but the current optically pumped configuration, though demonstrating high performance, does not fully exploit the wafer-scale fabrication and testing advantages of VCSELs. Referring to Figure 1, the ultimate low-cost electrically pumped MEMS-VCSEL swept source would eliminate the pump laser, pump isolator, WDM, and semiconductor optical amplifier. Elimination of the amplifier requires power levels of >10mW at 1060nm, which is a possible but a long-term goal. A nearer-term goal is elimination of pump laser, isolator, and WDM, leading to a pure electrically pumped device with a relatively low cost amplifier, still representing a major simplification relative to optical pumping.

Some of the challenges inherent in achieving widely tunable electrically pumped devices include reduction of cavity FSR due to thick intra-cavity current-spreading layers, and increased cavity losses due to dopants, which reduce gain, particularly far away from the gain peak where it is required for widely tunable devices. At 1060nm, these challenges can likely be overcome, due to the fact that 90-100nm tuning is likely adequate for most ophthalmic applications, 122nm has already been achieved in optically pumped devices, and compressively strained InGaAs quantum wells provide very high gain[29]. In addition, however, although single transverse mode operation is relatively easy to achieve in optical pumping using a single-mode pump beam and half-symmetric cavity[8], it is more challenging in electrical pumping. This is because creation of a current aperture for electrical pumping also creates a refractive index step, which can create strong lateral guiding and excite lateral transverse modes. As a result, careful attention must be paid to the method and placement of the current aperture, proper aperture size, and proper design of top mirror curvature in a half-symmetric cavity.

The first electrically pumped 1060nm MEMS VCSELs were reported by a Danish group in 2013[30], achieving 24 nm dynamic tuning range. Our group recently demonstrated 48.5 nm continuous tuning range and 67nm discontinuous tuning range at 1060nm. Figures 10A-B illustrate the basic device structure and our first tuning results. The device structure employs a 3-terminal configuration, in contrast to optical pumping which requires only two terminals to drive the MEMS actuator. As shown in Fig. 10A, the bottom MEMS contact functions also as the top contact for electrical injection into the gain region, while a third substrate contact serves as the bottom contact to the gain region. Figure 10B shows tuning results achieved to date, illustrating both static and dynamic spectra over a 67.2 nm tuning range, ultimately limited by the ~67.2nm free-spectral range (FSR) of the structure. The blue spectrum represents static operation at low MEMS voltage, while the red spectrum represents static operation with a higher MEMS voltage, which causes switching to the next longitudinal mode. Further application of DC bias plus AC voltage leads to the darker green time-averaged spectrum, demonstrating 48.5nm continuous tuning at 890kHz sinusoidal drive. The lighter green spectrum represents discontinuous dynamic tuning over 67.2 nm, or over the entire FSR, but using two longitudinal modes to cover the shorter and longer regions of this spectrum. The central peak in the light green spectrum is the region of overlap between short and long mode tuning. The 48.5 nm continuous tuning range is a more relevant measure than the 67.2nm discontinuous tuning for SS-OCT systems. A second transverse mode also appears at some wavelengths in the tuning range. This mode can be suppressed by further optimization of current aperture placement and size, as discussed above. The FSR can also be increased in future designs, to approach 100nm tuning. The results of Fig. 10B represent a significant step toward electrical pumping, and further improvements to tuning range and SMSR are anticipated in the coming year. We also anticipate imaging validation of these electrically pumped devices in the coming months.

7. CONCLUSION

Over the last two years, MEMS-VCSELs operating at 1060nm and 1300nm have emerged as a unique and high-performance swept source for SS-OCT imaging, demonstrating long coherence length, wide tuning range, and MHz range axial scan rates. Optically pumped devices have enabled high-performance imaging, including record high-speed endoscopic imaging, whole eye imaging, wide-field hand-held retinal imaging, ultra-long coherence length imaging, dye-free OCT angiography, and Doppler blood flow imaging.

Migration to electrical pumping remains an important future direction, promising to lower the cost of future SS-OCT systems. We report electrically pumped 1060nm MEMS-VCSELs with 48.5 nm continuous and 67.2 nm discontinuous tuning range. Further improvements to cavity design are expected to improve tuning range closer to those reported with optically pumped devices, and validation of electrically pumped devices in SS-OCT imaging is currently ongoing.

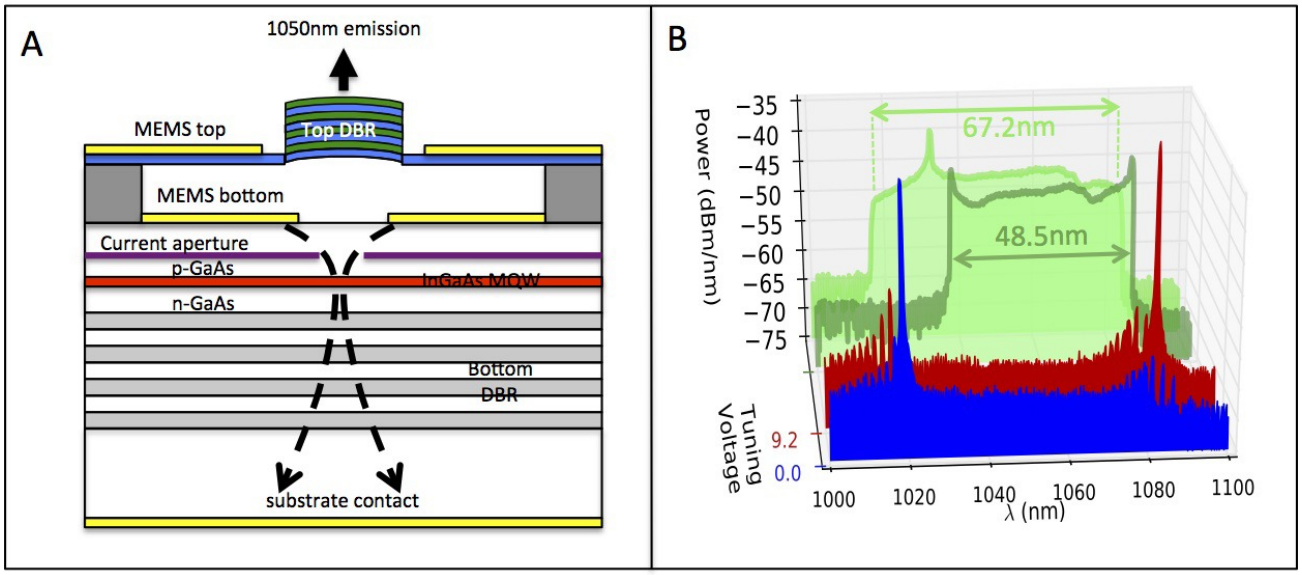

Figure 10: A. Electrically-pumped VCSEL structure showing 2 MEMS contacts and bottom substrate contact. Bottom MEMS contact and substrate contact accomplish electrical injection into InGaAs MQW gain region through current aperture, as illustrated by the dashed black lines. B. Tuning results demonstrating 48.5 continuous and 67.2 nm discontinuous dynamic tuning at 890kHz operation. The FSR is also ~67.2 nm, so this results represents full tuning over an entire FSR.

ACKNOWLEDGMENTS

This work was supported by commercial funding from Thorlabs and government funding from the National Institutes of Health and Air Force Office of Scientific Research (AFOSR) under the following grants and contracts: NIH R44EY022864-01,-02, NIH R44CA101067-05,-06,-07, R01-EY011289-26, R01-CA075289-15, R01-EY013178-12, R01-EY013516-09, R01-EY018184-05, R01-NS057476-05, AFOSR FA9550-10-1-0551 and FA9550-12-1-0499. The content is solely the responsibility of the authors and does not necessarily represent the views of the Air Force or the NIH.

REFERENCES

[1] Adler, D. C., Chen, Y., Huber, R. *et al.*, "Three-dimensional endomicroscopy using optical coherence tomography," Nature Photonics, 1(12), 709-716 (2007).

[2] Huber, R., Wojtkowski, M., Taira, K. *et al.*, "Amplified, frequency swept lasers for frequency domain reflectometry and OCT imaging: design and scaling principles," Optics Express, 13(9), 3513-3528 (2005).

[3] Grulkowski, I., Liu, J. J., Potsaid, B. *et al.*, "Retinal, anterior segment and full eye imaging using ultrahigh speed swept source OCTwith vertical-cavity surface emitting lasers," Biomed. Opt. Express, 3(11), 2733-2751 (2012).
[4] Potsaid, B., Jayaraman, V., Fujimoto, J. G. *et al.*, "MEMS tunable VCSEL light source for ultrahigh speed 60kHz - 1MHz axial scan rate and long range centimeter class OCT imaging," Proceedings of the SPIE - The International Society for Optical Engineering, 8213, (2012).
[5] Jayaraman, V., Jiang, J., Potsaid, B. *et al.*, "Design and performance of broadly tunable, narrow line-width, high repetition rate 1310nm VCSELs for swept source optical coherence tomography," Proceedings of the SPIE - The International Society for Optical Engineering, 8276, 82760D (11 pp.)-82760D (11 pp.) (2012).
[6] Larson, M. C., Massengale, A. R., and Harris, J. S., Jr., "Microelectromechanical wavelength-tunable vertical cavity laser," 1996. 54th Annual Device Research Conference Digest (Cat. No.96TH8193), 90-9191 (1996).
[7] Wu, M. S., Vail, E. C., Li, G. S. *et al.*, "Tunable micromachined vertical cavity surface emitting laser," Electronics Letters, 31(19), 1671-16721672 (1995).
[8] Matsui, Y., Vakhshoori, D., Peidong, W. *et al.*, "Complete polarization mode control of long-wavelength tunable vertical-cavity surface-emitting lasers over 65-nm tuning, up to 14-mW output power," IEEE Journal of Quantum Electronics, 39(9), 1037-10481048 (2003).
[9] Lackner, M., Schwarzott, M., Winter, F. *et al.*, "CO and CO 2 spectroscopy using a 60 nm broadband tunable MEMS-VCSEL at ap1.55 mum," Optics Letters, 31(21), 3170-31723172 (2006).
[10] Cole, G. D., Behymer, E., Bond, T. C. *et al.*, "Short-wavelength MEMS-tunable VCSELs," Optics Express, 16(20), 16093-16103 (2008).
[11] Huber, R., Adler, D. C., and Fujimoto, J. G., "Buffered Fourier domain mode locking: unidirectional swept laser sources for optical coherence tomography imaging at 370,000 lines/s," Optics Letters, 31(20), 2975-2977 (2006).
[12] Jayaraman, V., Chuang, Z. M., and Coldren, L. A., "THEORY, DESIGN, AND PERFORMANCE OF EXTENDED TUNING RANGE SEMICONDUCTOR-LASERS WITH SAMPLED GRATINGS," Ieee Journal of Quantum Electronics, 29(6), 1824-1834 (1993).
[13] George, B., and Derickson, D., "High-Speed Concatenation of Frequency Ramps Using Sampled Grating Distributed Bragg Reflector Laser Diode Sources for OCT Resolution Enhancement," Proceedings of the SPIE - The International Society for Optical Engineering, 7554, (2010).
[14] Jayaraman, V., Jiang, J., Li, H. *et al.*, "OCT Imaging up to 760 kHz Axial Scan Rate Using Single-Mode 1310nm MEMS-Tunable VCSELs with >100nm Tuning Range," CLEO: 2011 - Laser Science to Photonic Applications, 2 pp.-2 pp.2 pp. (2011).
[15] Jayaraman, V., Cole, G. D., Robertson, M. *et al.*, "Rapidly swept, ultra-widely-tunable 1060 nm MEMS-VCSELs," Electronics Letters, 48(21), 1331-1333 (2012).
[16] Jayaraman, V., Cole, G. D., Robertson, M. *et al.*, "High-sweep-rate 1310 nm MEMS-VCSEL with 150 nm continuous tuning range," Electronics Letters, 48(14), 867-9 (2012).
[17] MacDougal, M. H., Dapkus, P. D., Bond, A. E. *et al.*, "Design and fabrication of VCSELs with Al xO y-GaAs DBRs," IEEE Journal of Selected Topics in Quantum Electronics, 3(3), 905-915915 (1997).
[18] Dudley, J. J., Babic, D. I., Mirin, R. *et al.*, "Low-threshold, wafer fused long-wavelength vertical-cavity lasers," Applied Physics Letters, 64(12), 1463-1465 (1994).
[19] Black, A., Hawkins, A. R., Margalit, N. M. *et al.*, "Wafer fusion: Materials issues and device results," IEEE Journal of Selected Topics in Quantum Electronics, 3(3), 943-951 (1997).
[20] Jayaraman, V., Mehta, M., Jackson, A. W. *et al.*, "High-power 1320-nm wafer-bonded VCSELs with tunnel junctions," IEEE Photonics Technology Letters, 15(11), 1495-14971497 (2003).
[21] Gierl, C., Gruendl, T., Debernardi, P. *et al.*, "Surface micromachined tunable 1.55 mu m-VCSEL with 102 nm continuous single-mode tuning," Optics Express, 19(18), 17336-17343 (2011).
[22] Gierl, C., Gruendl, T., Zogal, K. *et al.*, "Surface micromachined MEMS-tunable VCSELs with wide and fast wavelength tuning," Electronics Letters, 47(22), 1243-1244 (2011).
[23] I. Grulkowski, J. J. L., J.Y. Zhang, B. Potsaid, V. Jayaraman, A.E. Cable, J.S. Duker, J.G. Fujimoto, "Reproducibility of a Long-Range Swept-Source Optical Coherence Tomography Ocular Biometry System and Comparison with Clinical Biometers," Ophthalmology, Article in Press DOI: 10.1016/j.ophtha.2013.04.007, (2013).

[24] WooJhon, C., Potsaid, B., Jayaraman, V. *et al.*, "Phase-sensitive swept-source optical coherence tomography imaging of the human retina with a vertical cavity surface-emitting laser light source," Optics Letters, 38(3), 338-40 (2013).
[25] Lu, C. D., Kraus, M. F., Potsaid, B. *et al.*, "Handheld ultrahigh speed swept source optical coherence tomography instrument using a MEMS scanning mirror," Biomedical Optics Express, 5(1), 293-311 (2014).
[26] Tsai, T.-H., Potsaid, B., Tao, Y. K. *et al.*, "Ultrahigh speed endoscopic optical coherence tomography using micromotor imaging catheter and VCSEL technology," Biomed. Opt. Express, 4(7), 1119-1132 (2013).
[27] Choi, W., Mohler, K. J., Potsaid, B. *et al.*, "Choriocapillaris and Choroidal Microvasculature Imaging with Ultrahigh Speed OCT Angiography," Plos One, 8(12), (2013).
[28] Grulkowski, I., Liu, J. J., Potsaid, B. *et al.*, "High-precision, high-accuracy ultralong-range swept-source optical coherence tomography using vertical cavity surface emitting laser light source," Optics Letters, 38(5), 673-675 (2013).
[29] Corzine, S. W., and Coldren, L. A., "Theoretical gain in compressive and tensile-strained InGaAs/InGaAsP quantum wells," Applied Physics Letters, 59(5), 588-590 (1991).
[30] Ansbaek, T., Chung, I.-S., Semenova, E. S. *et al.*, "1060-nm Tunable Monolithic High Index Contrast Subwavelength Grating VCSEL," IEEE Photonics Technology Letters, 25(4), 365-367 (2013).